

Scaling of an injection-controlled XeF(C#A) laser pumped by a repetitively pulsed, high current density electron beam

G. J. Hirst, C. B. Dane, W. L. Wilson, R. Sauerbrey, and F. K. TittelW. L. Nighan

Citation: *Appl. Phys. Lett.* **54**, 1851 (1989); doi: 10.1063/1.101256

View online: <http://dx.doi.org/10.1063/1.101256>

View Table of Contents: <http://aip.scitation.org/toc/apl/54/19>

Published by the [American Institute of Physics](#)

A close-up photograph of a single metal needle protruding from a large, textured pile of dry straw or hay. The background is a soft-focus field of similar straw, creating a strong visual metaphor for finding a needle in a haystack.

**FIND THE NEEDLE IN THE
HIRING HAYSTACK**

POST JOBS AND REACH THOUSANDS OF
QUALIFIED SCIENTISTS EACH MONTH.

PHYSICS TODAY | JOBS
WWW.PHYSICSTODAY.ORG/JOBS

Scaling of an injection-controlled XeF($C \rightarrow A$) laser pumped by a repetitively pulsed, high current density electron beam

G. J. Hirst, C. B. Dane, W. L. Wilson, R. Sauerbrey, and F. K. Tittel
Department of Electrical and Computer Engineering, Rice University, Houston, Texas 77251

W. L. Nighan
United Technologies Research Center, East Hartford, Connecticut 06108

(Received 16 January 1989; accepted for publication 1 March 1989)

This letter reports the design and performance of a scaled, injection-controlled XeF($C \rightarrow A$) laser pumped by a repetitively pulsed, high current density electron beam with a temporal duration of 10 ns full width at half maximum. Injection of a 2 mJ pulse at 486.8 nm having a spectral width of <0.005 nm resulted in an amplified output of 0.7 J corresponding to energy density and efficiency values of 1.5 J/ ℓ and 1.2%.

The XeF($C \rightarrow A$) laser is an efficient, pulsed radiation source, tunable throughout the entire blue-green region of the spectrum. It has been operated using a number of different pumping techniques including photolysis,¹ transverse electric discharges,² and short³ and long⁴ pulse electron beams. An Ar-Kr-Xe-NF₃-F₂ mixture, developed in this laboratory, pumped with a high current density (~ 250 A/cm²) electron beam of short duration [full width at half maximum (FWHM) ≈ 10 ns] results in a peak gain coefficient of $\sim 3\%$ cm⁻¹, allowing the laser to be efficiently injection controlled by a narrow band, tunable dye source with good beam quality. A tuning range of ~ 30 nm has been demonstrated using this approach, with laser energy density and intrinsic efficiency values of 1.5 J/ ℓ and 1.5%, respectively.³ The laser energy was limited to 20–30 mJ in these experiments by the small active volume (20 cm³). This letter reports the successful scaling of the XeF($C \rightarrow A$) laser volume, energy, and cavity magnification. Initial results are also presented from experiments in which the laser was operated at 0.1 Hz.

The design for a scaled XeF($C \rightarrow A$) laser was based on previous experimental results,³ detailed kinetic modeling,⁵ and an analytical model developed for injection-controlled excimer amplifiers.⁶ The goal was to build a laser with an energy output in the range 0.5–1 J. Previous experience indicated that an active volume and length of approximately 0.5 ℓ and 50 cm, respectively, combined with a deposited energy of 100 J/ ℓ , would be required to achieve these output levels. Analytical modeling provided the optimum resonator design for injection control. Using gain curves deduced from the performance of the small scale system operated with a similar electron beam pumping density, a laser output of 0.6 J was predicted for the scaled device with an unstable resonator magnification of 1.7 and an injection intensity of ~ 1 MW/cm², i.e., approximately one-fifth of the saturation intensity.

A schematic diagram of the experimental layout is shown in Fig. 1. The peak voltage and current of the electron beam, measured in the diode, are 550 kV and 83 kA, respectively, with a current pulse width of 10 ns FWHM measured in the laser cell. The machine can be operated continuously at repetition rates of up to 1 Hz. The electron beam enters the

laser cell through a 25 μ m titanium foil with a 5 μ m aluminum coating on the surface in contact with the laser gas. This leads to significantly improved gas lifetimes when compared with bare titanium foils. The cell and the gas handling system are otherwise made entirely from 316 stainless steel with Viton, Kel-F, and Teflon vacuum seals. In the experiments reported here the total laser gas pressure is 6.5 bar. The gas is introduced into the cell and is then mixed by circulating it through an external loop using a small bellows pump which, at this pressure, results in a flow rate of ~ 1 ℓ /min. The windows at each end of the cell are uncoated fused-silica flats. The active laser volume is 0.48 ℓ , as defined by the 3.5-cm-diam optical cavity and the 50 cm length pumped by the electron beam. Chlorostyrene film (Far West Technology, type 67-20) is used to measure the energy deposition in the active volume,⁷ a method that provides significantly higher accuracy and spatial resolution than is possible using the conventional pressure jump technique. The average volumetric energy deposition within this volume is measured to be 120 J/ ℓ .

The optical cavity consists of two fused-silica mirrors located inside the laser cell on adjustable mounts. The back reflector is plano-concave (radius of curvature = 2.73 m) with a 1.5-mm-diam hole drilled through its center to admit

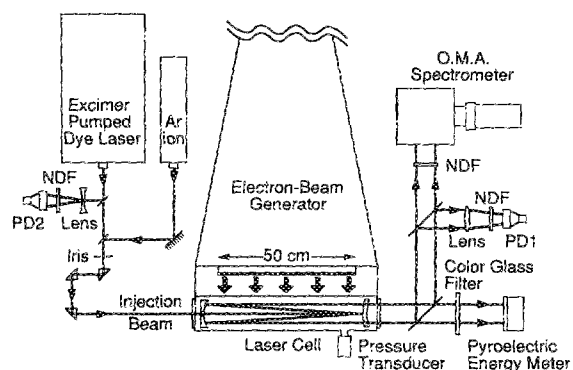


FIG. 1. Schematic diagram of the experimental layout. O.M.A.: optical multichannel analyzer, N.D.F.: neutral density filter, PD1 and PD2: vacuum photodiodes.

the injection beam. The concave surface is coated for maximum reflectivity ($>99\%$) between 465 and 505 nm. The reflectivity is minimized ($<15\%$) at 350 nm, the wavelength of the competing $\text{XeF}(B \rightarrow X)$ transition. The output coupler is a meniscus lens with radii of curvature of ± 1.61 m. The convex surface has a 2.1-cm-diam high-reflectance spot deposited on its center, while the concave surface is antireflection coated. The mirrors are located 56 cm apart, forming a positive-branch, confocal unstable resonator with a magnification of 1.7, the value calculated to optimize the near-field laser energy for the present conditions.

A dye laser pumped by a 60 ns XeCl laser provides a 40 ns FWHM injection source for the electron beam pumped amplifier. A 2 mJ pulse is delivered through the injection hole, corresponding to an input intensity of 3 MW/cm^2 . The dye laser is tuned to 486.8 nm, which is near the peak of the $\text{XeF}(C \rightarrow A)$ gain profile.⁸ The injection laser linewidth is less than 0.005 nm. An argon ion laser is also used for system alignment and for wavelength calibration.

The $\text{XeF}(C \rightarrow A)$ laser output is analyzed using two vacuum photodiodes, a pyroelectric energy meter, and an optical multichannel analyzer/spectrometer combination with a resolution of 0.25 nm. The photodiode PD1 (see Fig. 1) is used to monitor the temporal shape of the amplifier output. The signal from PD2 is used to confirm correct temporal synchronization between the injection laser and the electron beam pulse, and also to measure the energy injected into the amplifier. The amplified output passes through a CS 3-74 color glass filter which absorbs any ultraviolet light before energy measurements are made. System diagnostics include voltage and current monitors on the electron beam machine and a pressure transducer coupled to the laser cell. This allows the change in cell pressure to be measured when the machine is fired.

The experimental sequence of arming the diagnostics, triggering the lasers, and acquiring and displaying the results is managed by a PC AT compatible microcomputer. The computer system is housed in a Faraday cage and is coupled to the control and data acquisition hardware (located in a separate shielded enclosure) using optical fibers to avoid electromagnetic interference when the electron beam machine is fired.

Figure 2 shows spectra of the laser output taken with three different optical configurations. Figure 2(a) presents the UV/visible fluorescence observed along the optical axis in the absence of the internal resonator mirrors, but with the two silica windows aligned. The spectrum shows a strong peak at the $\text{KrF}(B \rightarrow X)$ wavelength of 249 nm. A weaker feature at 351–353 nm is due to fluorescence on the $\text{XeF}(B \rightarrow X)$ transition. On the scale of the peak UV signal, the broadband $\text{XeF}(C \rightarrow A)$ fluorescence is barely visible in the region around 480 nm, although it becomes more apparent when the vertical scale is magnified by a factor of 10.

Figure 2(b) shows the effect of mounting the unstable resonator optics inside the laser cell. In the absence of an injected pulse, the free-running laser exhibits a broadband output from 465 to 505 nm, with sharp absorption features attributed to excited rare-gas atomic species.³ The amplified spontaneous emission on the two $B \rightarrow X$ transitions is domi-

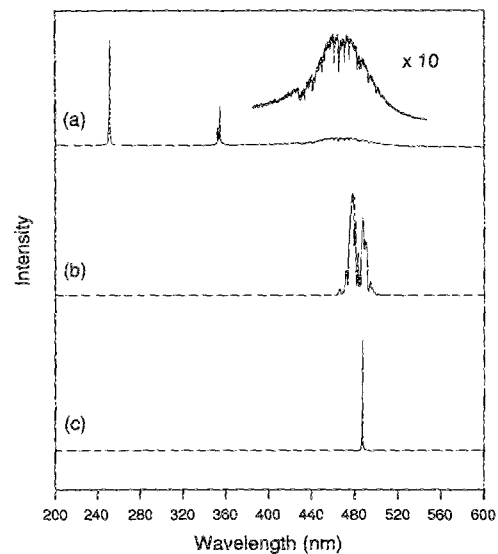


FIG. 2. Spectrally resolved output from the $\text{XeF}(C \rightarrow A)$ laser for three different optical configurations: (a) fluorescence along the optical axis in the absence of laser mirrors, but with the cell windows aligned, (b) laser output with mirrors but with no injected pulse, (c) amplifier output with the injection of a 486.8 nm pulse having a spectral width of <0.005 nm.

nated by the $\text{XeF}(C \rightarrow A)$ output following the addition of the cavity. The use of a higher partial pressure of krypton than in previous experiments³ (see Table I) facilitates the suppression of the $\text{KrF}(B \rightarrow X)$ output. The $\text{XeF}(C \rightarrow A)$ laser energy, corrected for losses due to the cell window, the first beamsplitter, and the filter, is ~ 0.1 J under these conditions.

Figure 2(c) shows the spectral output when the amplifier is operated with a 2 mJ injection pulse (3 MW/cm^2). An intense, narrow line at the injection wavelength of 486.8 nm is observed. The displayed linewidth is spectrometer-limited; however, previous experience³ has shown that the amplified output has the same spectral width as the injected pulse, i.e., <0.005 nm. The output pulse duration is 10 ns FWHM. The measured output energy for these conditions is 0.7 J, in good agreement with the predicted value. The corresponding extracted energy density is 1.5 J/l and the intrinsic laser efficiency is 1.2%.

TABLE I. Experimental conditions and results.

Input energy density, peak power	120 J/l, 12 MW/cm ²
Electron beam pulse duration	10 ns (FWHM)
Electron beam current density	$\sim 250 \text{ A/cm}^2$ at foil
Extracted optical volume, length	0.48 l, 50 cm
Resonator magnification	1.7
Gas composition	
F ₂	1.3 mbar
NF ₃	10.5 mbar
Xe	10.5 mbar
Kr	1.6 bar
Ar	4.9 bar
Laser output energy, energy density	0.7 J, 1.5 J/l
Intrinsic efficiency	1.2%

Figure 3 shows the results of an experiment designed to study the repetitively pulsed XeF($C \rightarrow A$) system. The injection-controlled laser is fired at a repetition rate of 0.1 Hz and two pyroelectric energy meters are used to measure the total output energy and the output in the blue green. Spectrometer measurements reveal that the difference between these signals is due to KrF($B \rightarrow X$) laser action. The energies at 487 and 249 nm are plotted as functions of time, starting with a fresh gas fill. After 50 shots the machine is halted for 10 min and a single shot is then fired to measure the gas recovery.

It can be seen that the ultraviolet laser is initially very weak (less than 20 mJ for the first three shots) but that it subsequently begins to rise at the expense of the blue-green signal. After 50 shots the output at 249 nm exceeds 0.1 J while that at 487 nm has fallen from slightly over 0.6 J to approximately 0.45 J. Gas circulation for a period of 10 min restores the XeF($C \rightarrow A$) energy to 0.54 J and reduces the KrF($B \rightarrow X$) output to 75 mJ.

The behavior of the repetitively pulsed output can be explained by considering the properties of the gas circulation system, which was not designed for repetitive operation of the laser. The total gas volume is 4ℓ, of which approximately 1 ℓ is pumped by the electron beam on each shot. The gas flow rate (~ 1 ℓ/min) is too slow for complete gas mixing between shots. The changes in the laser output are probably due to reaction products produced in the pumped region. Since the gas flow rate is low, their concentration will remain higher there than in the rest of the gas volume, causing the output to change more rapidly than it otherwise would. The partial recovery after a period of circulation reflects the effects of more thorough gas mixing. Changes in the laser output can be reduced by improving the circulation system and by increasing the unpumped gas volume.

The results of these experiments show that the electron beam pumped XeF($C \rightarrow A$) laser can be operated continuously at 0.1 Hz, with only a slow, systematic decrease in output energy due probably to changes in gas chemistry. At present the laser output energy at a 1 Hz repetition rate is limited by transient gas turbulence effects. It is believed that these can be remedied by the addition of a fast-flow gas handling system.

In conclusion, we have demonstrated efficient scaling of the XeF($C \rightarrow A$) laser in the short-pulse (10 ns) pumping regime, and have obtained very encouraging initial results concerning the repetitive operation of this system. The applicability of an analytical model to the scaling of the device has been demonstrated and it has been shown that despite the significant increase in the length of the gain-medium, lasing on the rare-gas halide $B \rightarrow X$ transitions can be suppressed by

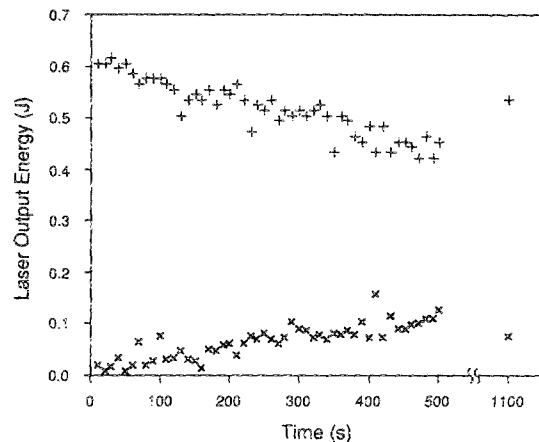


FIG. 3. Energy per pulse on the XeF($C \rightarrow A$) transition at 486.8 nm (+) and the KrF($B \rightarrow X$) transition at 249 nm (x) for 50 consecutive laser pulses, taken at a 0.1 Hz repetition rate.

an appropriate choice of gas mixture and optics. Injection control at 486.8 nm of the electron beam pumped amplifier resulted in an output energy of 0.7 J, representing an intrinsic laser efficiency of 1.2% and an extraction energy density of 1.5 J/ℓ. Moreover, it is anticipated that this level of amplifier performance can be maintained for injection wavelengths throughout the 460–510 nm region.

We wish to acknowledge productive interactions with the staff at Maxwell Laboratories, Inc., the builders of the electron beam machine. Helpful conversations with Dr. I. J. Bigio and the technical support of J. Hooten are much appreciated. This work was supported by the Office of Naval Research, the National Science Foundation, and the Robert Weich Foundation.

¹D. J. Eckstrom and H. C. Walker, *IEEE J. Quantum Electron.* **18**, 176 (1982); V. S. Zuev, G. N. Kashnikov, N. P. Kozlov, S. B. Mamaev, V. K. Orlov, Yu. S. Protasov, and V. A. Sorokin, *Sov. J. Quantum Electron.* **16**, 1665 (1986).

²H. Voges and G. Marowsky, *IEEE J. Quantum Electron.* **24**, 827 (1988); R. C. Hollins, D. L. Jordan, and A. Feltman, *Opt. Comm.* **63**, 61 (1987).

³N. Hamada, R. Sauerbrey, W. L. Wilson, F. K. Tittel, and W. L. Nighan, *IEEE J. Quantum Electron.* **24**, 1571 (1988).

⁴A. Mandl and L. N. Litzenberger, *Appl. Phys. Lett.* **53**, 1690 (1988).

⁵W. L. Nighan and M. C. Fowler, *IEEE J. Quantum Electron.* (1989) (to be published).

⁶N. Hamada, R. Sauerbrey, and F. K. Tittel, *IEEE J. Quantum Electron.* **24**, 2458 (1988).

⁷W. P. Bishop, K. C. Humpherys, and P. K. Randtke, *Rev. Sci. Instrum.* **44**, 443 (1973).

⁸F. K. Tittel, G. Marowsky, W. L. Nighan, Y. Zhu, R. Sauerbrey, and W. L. Wilson, *IEEE J. Quantum Electron.* **22**, 2168 (1986).